GEOPHYSICAL RESEARCH LETTERS, VOL. 37, L07201, doi:10.1029/2009GL041642, 2010

First high-resolution stratigraphic column of the Martian north polar layered deposits

Kathryn E. Fishbaugh,[1] Christine S. Hvidberg,[2] Shane Byrne,[3] Patrick S. Russell,[1] Kenneth E. Herkenhoff,[4] Mai Winstrup,[2] and Randolph Kirk[4]

Received 19 November 2009; revised 23 January 2010; accepted 17 February 2010; published 2 April 2010.

[1] This study achieves the first high-spatial-resolution, layer-scale, measured stratigraphic column of the Martian north polar layered deposits using a 1m-posting DEM. The marker beds found throughout the upper North Polar Layered Deposits range in thickness from 1.6 m–16.0 m +/– 1.4 m, and 6 of 13 marker beds are separated by ~25–35 m. Thin-layer sets have average layer separations of 1.6 m. These layer separations may account for the spectral-power-peaks found in previous brightness-profile analyses. Marker-bed layer thicknesses show a weak trend of decreasing thickness with depth that we interpret to potentially be the result of a decreased accumulation rate in the past, for those layers. However, the stratigraphic column reveals that a simple rhythmic or bundled layer sequence is not immediately apparent throughout the column, implying that the relationship between polar layer formation and cyclic climate forcing is quite complex. **Citation:** Fishbaugh, K. E., C. S. Hvidberg, S. Byrne, P. S. Russell, K. E. Herkenhoff, M. Winstrup, and R. Kirk (2010), First high-resolution stratigraphic column of the Martian north polar layered deposits, *Geophys. Res. Lett.*, *37*, L07201, doi:10.1029/2009GL041642.

1. Introduction

[2] The participants of the 4th International Mars Polar Science and Exploration Conference posed the following as one of the most important questions in the field: "What chronology, compositional variability, and record of climatic change is expressed in the stratigraphy of the polar deposits?" [*Fishbaugh et al.*, 2008]. The answer to this question has consequences reaching far beyond the Mars polar community in its implications for past, recent climate history. Fully utilizing the climatic information stored within the polar stratigraphic record is a two-step process. Firstly, the stratigraphic record itself must be accurately described, a process hindered to date by the absence of topographic data at the scale of individual layers and the use of brightness to delineate individual layers (a property we now know to be ambiguous at best [*Herkenhoff and Murray*, 1990; *Herkenhoff et al.*, 2007; *Fishbaugh et al.*, 2010]). The second step is to utilize this polar stratigraphic record as a constraint on climatic models. For example, one can construct a layer accumulation model [e.g., *Levrard et al.*, 2004] wherein parameters that control the deposition of layers, such as climate forcing-related to obliquity and precession-and dust cycles, can be adjusted to match the measured thicknesses and elevations of known layer types; portions that do not match could lead to inferences about more stochastic events like dust storms, ice flow, or prolonged erosion. Here in this paper, we concentrate on furthering the first of these steps by constructing the first stratigraphic column of the upper few hundred meters of Martian north polar stratigraphy.

[3] Many previous authors have analyzed various image datasets in efforts to classify large-scale, broad layer types [*Murray et al.*, 1972; *Cutts et al.*, 1976; *Howard et al.*, 1982; *Milkovich and Head*, 2006], search for dominant brightness-frequencies (with respect to depth) [*Milkovich and Head*, 2005; *Perron and Huybers*, 2009; *Milkovich et al.*, 2009], and correlate major layers within the north and south PLD (based on their brightness and lower resolution morphology) [*Fenton and Herkenhoff*, 2000; *Kolb and Tanaka*, 2001; *Herkenhoff et al.*, 2002, 2003; *Byrne and Ivanov*, 2004; *Fishbaugh and Hvidberg*, 2006; *Kolb and Tanaka*, 2006; *Milkovich et al.*, 2008; *Milkovich and Plaut*, 2008]. DEMs derived from Mars Orbiter Camera (MOC) photoclinometry have allowed measurements of 20–40 m thick layers and comparisons of these measurements from one location to another [*Herkenhoff et al.*, 2006]. But due to the lack of higher resolution topography and imagery, no previous studies have been able to characterize and classify individual layer types by their detailed morphology and measure their thicknesses at ~1 m scales. The major advance presented in this study builds on the work of *Fishbaugh et al.* [2010] to incorporate the finest-scale division of PLD stratigraphy possible from orbit, topographic measurements of true, individual layer thicknesses, and morphologic interpretation of layer types into a continuous, measured stratigraphic column. This study further serves to illustrate the type of information that may be expected from future HiRISE polar DEMs.

[4] The study area covers a 400 m vertical section within *Tanaka et al.*'s [2008] Planum Boreum 1 unit (ABb_1). This site was chosen by the HiRISE team for the first NPLD DEM because some of the major layers exposed here are known (from MOC images) to be representative of much of the top ~500 m of the NPLD [*Milkovich and Head*, 2005; *Fishbaugh and Hvidberg*, 2006; *Milkovich et al.*, 2009]. First, we briefly describe qualitative analysis of layer stratigraphy and classification of layer types. We then detail the

[1] Center for Earth and Planetary Studies, Smithsonian National Air and Space Museum, Washington, D. C., USA.
[2] Center for Ice and Climate, Niels Bohr Institute, University of Copenhagen, Copenhagen, Denmark.
[3] Lunar and Planetary Laboratory, University of Arizona, Tucson, Arizona, USA.
[4] U.S. Geological Survey, Flagstaff, Arizona, USA.

0094-8276/10/2009GL041642

methods used in the construction of the stratigraphic column and discuss the results of the derived stratigraphy, including how layer thicknesses and separation distances vary with depth.

2. Methods

[5] For all morphometric measurements reported herein, we use a 1m/pixel scale, ~30 cm vertical accuracy DEM, created from HiRISE stereo pair PSP_001738_2670 and PSP_001871_2670 at 87.1°N, 92.6°E [*McEwen et al.*, 2007; *Kirk et al.*, 2008; *Fishbaugh et al.*, 2010] (see Figure S1 of the auxiliary material for location map).[1] We use these summertime HiRISE images for qualitative analysis of layer morphology and consequent layer identification and classification.

2.1. Layer Types

[6] Two main layer types have previously been characterized throughout the upper NPLD. *Fishbaugh et al.* [2010] have discovered several layers that they term "marker beds" [see *Fishbaugh et al.*, 2010, Figures 9 and 10] because of their distinct (easily recognized), prominent (protrude from the other layers) morphology, similar to that of the well-known, original maker bed discovered by *Malin and Edgett* [2001]. These marker beds have hummocky (sometimes upturned [*Herkenhoff et al.*, 2006]) layer edges and linear, erosional fluting and pitting on their surfaces. Often, marker beds are darker than the other layers, whether due to having a higher inherent dust content or to collecting/retaining more surface dust/less surface frost. Sets of distinct, erosionally resistant thin layers between the marker beds have also been observed [*Milkovich and Head*, 2006; *Fishbaugh et al.*, 2010]. These thin layers (~1.5 m each, see table in Figure S3) protrude from adjacent materials, are relatively smooth in appearance, are traceable for long distances in one image and, as described below, tend to occur in couplets with less-resistant layers. Thus, the thin-layer sets are not likely to simply be thin marker beds, but they and the marker beds are the only distinguishable, traceable layer types. In our study outcrop, we place the identified layers into a known stratigraphic context by labeling the layers previously identified in MOC images as part of an NPLD-wide sequence [*Fishbaugh and Hvidberg*, 2006]. Identifiable layers are separated by material that cannot be differentiated into separate layers, often due to younger mantle deposits or other modification. Some of this undifferentiable material appears to be highly modified thin-layer sets, but the layers are not easily traceable across the outcrop.

2.2. Layer Thickness and Separation Measurements

[7] Using a technique described by *Fishbaugh et al.* [2010], we mark morphological layer boundaries using the HiRISE images from the stereo pair and a shaded relief map created from the DEM. Elevations of these boundaries are extracted from the DEM in ESRI's ArcMap, and the elevation of each boundary is obtained from an average of ~100 measurements lying along a straight line (~100 m long) that represents a smoothed version of the layer boundary (removing small-scale roughness resulting from surface irregularities or modification). Please see the auxiliary material for calculation of errors.

[8] The thin-layer sets appear to consist of multiple couplets, each of which is composed of the thin resistant ice-dust layer and a less erosionally-resistant ice-dust mixture of similar apparent thickness. Given resolution limits, we have only noted the elevation of the middle of each individual thin layer, and thus the separations between the middles of thin layers, a measurement that happens to be very close to the apparent thicknesses of the thin layers.

3. Results and Discussion

3.1. Stratigraphic Column

[9] The table in Figure S2 presents the results of the layer thickness and separation distance measurements, and we have compiled these results into the stratigraphic column in Figure 1a. Because the original marker bed is easily recognized [*Malin and Edgett*, 2001] and has been mapped across the NPLD by several authors [*Milkovich and Head*, 2005; *Fishbaugh and Hvidberg*, 2006], we label it as "MB" and label all other marker beds as MB − x or MB + x, depending on whether they lie stratigraphically below the MB or above it. Layers definitively identified as marker beds are labeled in orange, layers that are likely marker beds but have been somewhat obscured by mantling deposits or changing slope are in green, sets of thin layers are in blue, and sections that could not be confidently differentiated into separate layers are in grey. Notably, a simple rhythmic layer sequence is not immediately apparent, and marker beds and thin layer sets are not obviously grouped together. In this respect, the stratigraphic patterns of the polar layers are much more complicated than the regular patterns in sedimentary rocks at lower latitudes, for example, in Arabia Terra where layer sequences are bundled rhythmically into larger units at a ratio of 1:10 [*Lewis et al.*, 2008].

[10] Although the current results explicitly apply only to this location, several clues suggest that this stratigraphic column may be qualitatively representative of the upper 400 m of the NPLD in the main Planum Boreum dome, even while exact layer thicknesses and separations may vary somewhat. *Fishbaugh and Hvidberg* [2006] have correlated several of these layers across the NPLD using MOC images, and as Figure 1e shows, the high resolution stratigraphic sequence evident in HiRISE images is also present in outcrops separated from the study location by 90° in longitude (230 km). Additionally, sounding radar data from MRO's Shallow Subsurface Radar (SHARAD) and Mars Express' Mars Advanced Radar for Subsurface and Ionosphere Sounding (MARSIS) show continuous radar layering (at scales of 10s of meters in thickness) across the upper section of the NPLD [*Phillips et al.*, 2008; *Putzig et al.*, 2009].

3.2. Layer Separations

[11] With only one DEM of the upper NPLD having yet been produced, and with only 13 marker beds within that stratigraphic section, it is not possible to produce a robust statistical analysis of NPLD layer separations or thicknesses. HiRISE DEMs are time-consuming to produce, and this DEM is the first of its kind, providing invaluable insight into the high resolution details of NPLD stratigraphy, so we focus here on what can be concluded from one DEM, with the caveat that the addition of future DEMs may change or

[1] Auxiliary materials are available in the HTML. doi:10.1029/2009GL041642.

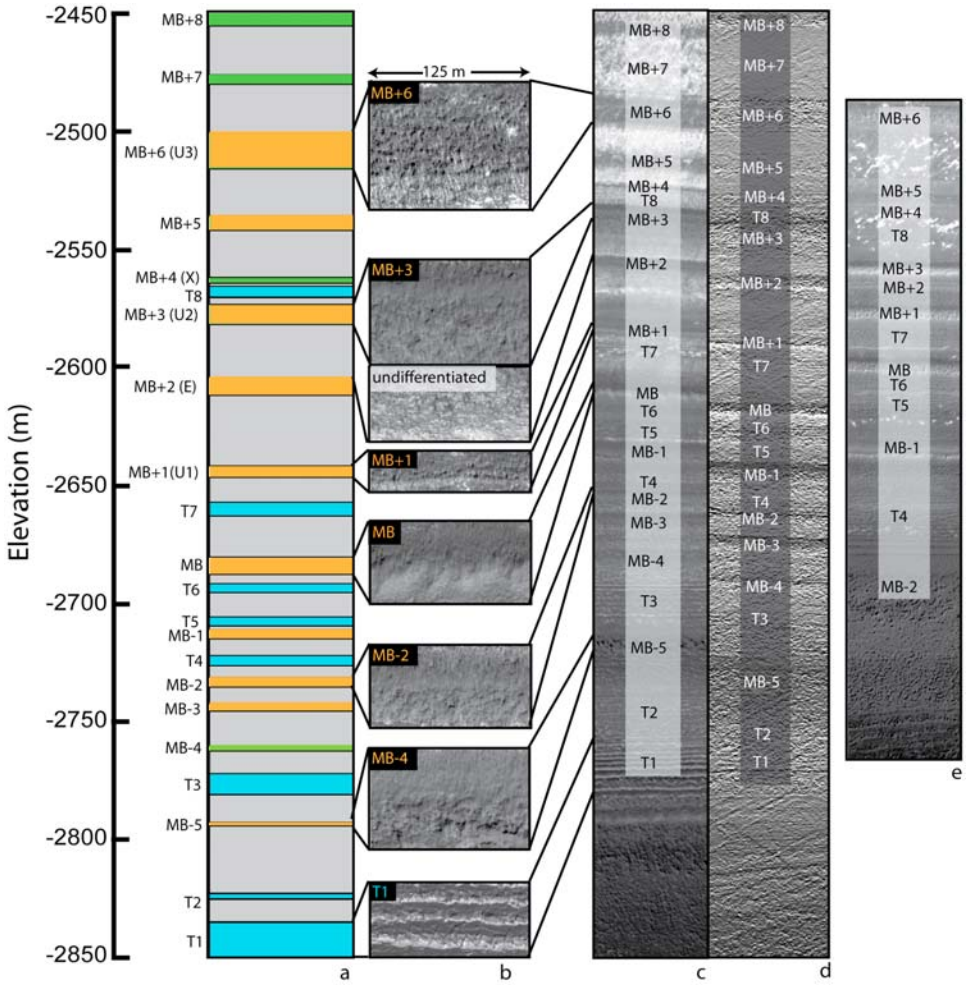

Figure 1. See Figure S1 for location and context. (a) Stratigraphic column created by measuring the thicknesses of layers in the DEM. Scale on left is elevation in meters. Layer labels in parentheses are those identified by *Fishbaugh and Hvidberg* [2006]. Colors are explained in the text. (b) Examples of layer morphology, labeled in the same way as in Figure 1a. (c) Portion of HiRISE image PSP_001738_2670, with layers labeled as in Figure 1a. (d) Portion of shaded relief map created from the DEM, with layers labeled as in Figure 1a. (e) Portion of HiRISE image PSP_001616_2670 located at 87.0°N, 175.4°E, approximately 90° east of the DEM, with layers labeled as in Figure 1a. Elevation scale on left does not apply to this image. Illumination for all images is from the lower right. Shaded relief has same illumination conditions as the images.

refine the quantitative results. From the table in Figure S2, one can see signs of interesting patterns whose regional prevalence and statistical significance can be improved upon with future DEMs. Six of the thirteen marker beds have separation distances of approximately 24–36 m. *Milkovich and Head* [2005] and *Milkovich et al.* [2008], through Fourier analysis of layer-brightness profiles (affected by surficial frost and topography), noted peak wavelengths of 24 to 35 m throughout the upper NPLD. From the table in Figure S3, the separation between the thin layers averages ~1.6 m. *Perron and Huybers* [2009] detected a rise in spectral power at 1.6 m using spectral wavelet analysis in several places across the NPLD. Thus, by categorizing layer types and placing them within a measured stratigraphic column, we may have identified the geologic features responsible for the characteristic brightness vs. depth frequencies reported previously [*Milkovich and Head*, 2005; *Milkovich et al.*, 2008; *Perron and Huybers*, 2009].

3.3. Thinning With Depth

[12] Close examination of Figure 1a reveals that, except for T1, and T3, the marker beds and thin-layer sets each show a weak thinning with depth (Figure 2a). Focusing on the trend rather than the major exceptions, several potential causes for thinning with depth, acting individually or in concert, are observational effects, i.g.: 1) observational bias due to shallower slopes at depth, 2) increasing layer dip angle with depth; and/or physical processes, i.g.: 1) layer thinning resulting from ice flow in the past (due to, e.g., past high temperatures at higher obliquity), 2) layer thinning resulting from compaction over time, and 3) a lower net accumulation rate in the past (due, e.g., to such factors as higher past temperatures or lower atmospheric water content - determining specific factors requires detailed modeling beyond the scope of this paper). Additionally, stochastic events, such as melting, impacts, and dust storms, can complicate layer thicknesses and separations, but will likely

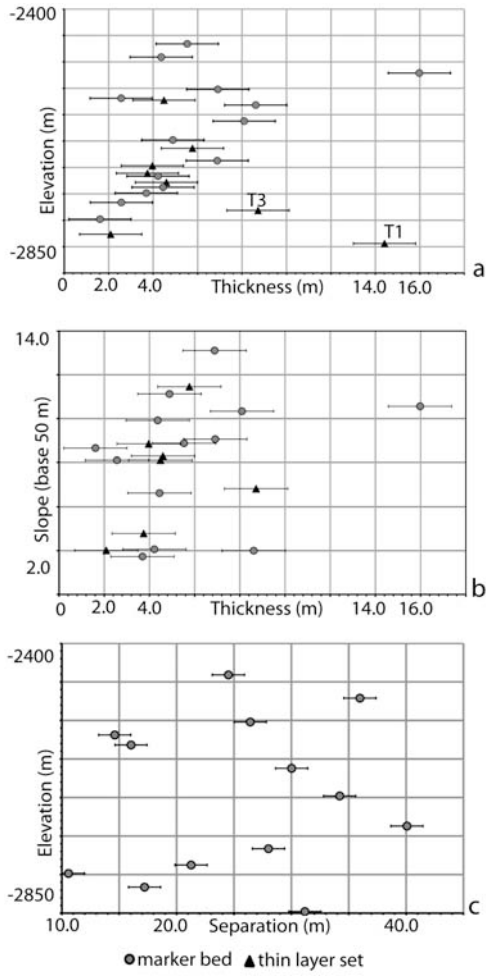

Figure 2. (a) Layer thickness versus elevation of middle of each layer. Note that thicknesses of the thin layer sets are representative of the entire set, not each, individual layer. Grey circles, marker beds; black triangles, thin layer sets. (b) Layer thickness versus trough wall slope (perpendicular to the layer strike) on a 50 m baseline. (c) Separation between marker beds versus the elevation of the middle of each layer.

cause exceptions to a general trend, rather than changing the trend.

[13] To assess the potential observational effects, we have plotted layer thickness as a function of average slope of the trough wall (the outcrop surface) on a 50 m baseline (Figure 2b) and have estimated the dip of the MB + 6 layer (the thickest marker bed, high in the sequence) and the MB − 3 layer (the thinnest marker bed, low in the sequence). There is no obvious trend of decreasing layer thickness with decreasing slope, so there appears to be little to no observational bias produced by shallow slopes exposing thin layers more readily than do steeper slopes. Also, assuming that a layer's upper boundary line in the outcrop is a trace of the upper bounding plane of the layer and that the orientation of the layer does not vary significantly across the outcrop, one can use the curve in the trough wall to obtain elevation measurements at different points on the plane of the layer's upper surface and calculate the dip of the plane. The dips of the MB + 6 and MB − 3 layers are less than 1.3°, so dip has very little effect on measured layer thickness in this outcrop. This result is consistent with the 1° dips measured using DEMs created from MOC photoclinometry [*Herkenhoff et al.*, 2006].

[14] In assessing the potential physical processes, we note that the separation distance between the marker bed layers does not decrease with depth (Figure 2c), making unlikely the possibility that layer thinning with depth is due to ice flow or to compaction of the PLD. However, if the marker beds have a fundamentally different composition from the rest of the PLD that has made them weaker or initially more porous, they may be more easily compacted; but their relatively high erosional resistance would argue against this.

[15] Two observations argue against an overall lower net accumulation rate in the past: 1) there are exceptions to the general decrease of layer thickness with depth and 2) the separation between marker beds shows no trend with depth. However, it is possible that only the marker beds have experienced some increase in net accumulation rate with time, though we would not assert that this has been a strong or linear trend. It is beyond the scope of this paper to explain why the marker beds may have experienced a weak trend in accumulation rate not experienced by the rest of upper NPLD or to explain why the trend has a particular (though weak) direction. We speculate that, if this trend is indeed borne out by future DEMs, it may have to do with the marker beds forming under different environmental conditions from the other layers, consistent with their distinctive morphology. For example, if the marker beds have formed as a lag deposit during times of net ablation, their thicknesses would be related to not just simple accumulation of ice/dust, but rather the amount of ice/dust ablated, the ice/dust ratio of that ablated material, and the amount of time needed for ice to again fill most/all of the lag pore space.

4. Conclusions

[16] We have created the first high-resolution, layer-scale, measured stratigraphic column of the NPLD; this column spans layers of the upper 400 m and is likely characteristic, at least qualitatively, of the upper NPLD in the main Planum Boreum dome. Layers can be categorized into marker beds, thin-layer sets, and sections that cannot be differentiated due to surface modification. The 13 marker beds have a range of thicknesses, from 1.6–16.0 ± 1.4 m, and do not appear to be grouped into clusters, but do show a weak trend of decreasing thickness with depth. The separation distances between six of the marker beds is about 24–36 m, and the average separation between the thin layers is ~1.6 m. We have thus likely identified the physical geological features that are responsible for the widespread dominant brightness-wavelengths of 24–35 m, discovered by *Milkovich and Head* [2005] and *Milkovich et al.* [2008], and 1.6 m, found by *Perron and Huybers* [2009]. Significantly, our results show that the upper NPLD does not include any simple cyclic inter-layering or bundling of marker beds and thin layers. This finding implies that the linkage between polar stratigraphy and cyclic climate forcing is complex and defies simply tying particular layers to particular peaks in these forcers (as attempted by *Laskar et al.* [2002]). The current findings and analysis provide the first synthesized illustration of what can be discerned in the NPLD using HiRISE DEMs. Further analysis of future DEMs at different

locations within the same stratigraphic section will be necessary to lend statistical confidence to the trends observed here and to assess variability over the whole NPLD.

[17] **Acknowledgments.** This work was funded by a NASA Mars Reconnaissance Orbiter Participating Scientist grant to KEF. The DEM was created at the USGS Astrogeology Science Center in Flagstaff, AZ. Thanks are gratefully extended to the International Space Science Institute (ISSI) in Bern, Switzerland for hosting the KEF-led team, "Are the Martian polar deposits a Rosetta Stone for the climate?"; the fruitful discussions during those meetings greatly improved our understanding of the NPLD stratigraphy. CSH thanks the Danish Council for Independent Research for support.

References

Byrne, S., and A. B. Ivanov (2004), Internal structure of the Martian south polar layered deposits, *J. Geophys. Res.*, *109*, E11001, doi:10.1029/2004JE002267.

Cutts, J., K. Blasius, G. Briggs, M. Carr, R. Greeley, and H. Masursky (1976), North polar region of Mars: Imaging results from Viking 2, *Science*, *194*, 1329–1337 doi:10.1126/science.194.4271.1329.

Fenton, L., and K. Herkenhoff (2000), Topography and stratigraphy of the Martian north polar layered deposits using photoclinometry, stereogrammetry, and MOLA altimetry, *Icarus*, *147*, 433–443, doi:10.1006/icar.2000.6459.

Fishbaugh, K., and C. Hvidberg (2006), Martian north polar layered deposits stratigraphy: Implications for accumulation rates and flow, *J. Geophys. Res.*, *111*, E06012, doi:10.1029/2005JE002571.

Fishbaugh, K., et al. (2008), Introduction to the 4th Mars Polar Science and Exploration Conference special issue: Five top questions in Mars polar science, *Icarus*, *196*, 305–317, doi:10.1016/j.icarus.2008.05.001.

Fishbaugh, K., S. Byrne, K. Herkenhoff, R. Kirk, C. Fortezzo, P. Russell, and A. McEwen (2010), Evaluating the meaning of "layer" in the Martian north polar layered deposits and the impact on the climate connection, *Icarus*, *205*, 269–282, doi:10.1016/j.icarus.2009.04.011.

Herkenhoff, K. E., and B. C. Murray (1990), High-resolution topography and albedo of the south polar layered deposits on Mars, *J. Geophys. Res.*, *95*, 14,511–14,529, doi:10.1029/JB095iB09p14511.

Herkenhoff, K., L. Soderblom, and R. Kirk (2002), MOC Photoclinometry of the north polar residual cap on Mars, *Lunar Planet. Sci.*, *XXXIII*, Abstract 1714.

Herkenhoff, K., L. Soderblom, and R. Kirk (2003), Stratigraphy and structure of the south polar layered deposits on Mars, paper presented at the Third International Conference on Mars Polar Science and Exploration, Lunar Planet. Inst., Alberta, Ont., Canada, 13–17 Oct.

Herkenhoff, K. E., L. A. Soderblom, R. L. Kirk, L. Keszthelyi, T. Becker, and L. Weller (2006), Stratigraphy and structure of the north polar layered deposits on Mars, paper presented at the Fourth International Conference on Mars Polar Science and Exploration, Lunar Planet. Inst., Davos, Switzerland, 2–6 Oct.

Herkenhoff, K., S. Byrne, P. Russell, K. Fishbaugh, and A. McEwen (2007), Meter-scale morphology of the north polar region of Mars, *Science*, *317*, 1711–1715, doi:10.1126/science.1143544.

Howard, A., J. Cutts, and K. Blasius (1982), Stratigraphic relationships within the Martian polar cap deposits, *Icarus*, *50*, 161–215, doi:10.1016/0019-1035(82)90123-3.

Kirk, R. L., et al. (2008), Ultrahigh resolution topographic mapping of Mars with MRO HiRISE stereo images: Meter-scale slopes of candidate Phoenix landing sites, *J. Geophys. Res.*, *113*, E00A24, doi:10.1029/2007JE003000.

Kolb, E., and K. Tanaka (2001), Geologic history of the polar regions of Mars based on Mars Global Surveyor data: II. Amazonian period, *Icarus*, *154*, 22–39, doi:10.1006/icar.2001.6676.

Kolb, E., and K. Tanaka (2006), Accumulation and erosion of south polar layered deposits in the Promethei Lingula region, Planum Australe, Mars, *Mars*, *2*, 1–9.

Laskar, J., B. Levrard, and F. Mustard (2002), Orbital forcing of the Martian polar layered deposits, *Nature*, *419*, 375–377, doi:10.1038/nature01066.

Levrard, B., F. Forget, F. Montmessin, and J. Laskar (2004), Recent ice-rich deposits formed at high latitudes on Mars by sublimation of unstable equatorial ice during low obliquity, *Nature*, *431*, 1072–1075, doi:10.1038/nature03055.

Lewis, K., O. Aharonson, J. Grotzinger, R. Kirk, A. McEwen, and T.-A. Suer (2008), Quasi-periodic bedding in the sedimentary rock record of Mars, *Science*, *322*, 1532–1535 doi:10.1126/science.1161870.

Malin, M. C., and K. S. Edgett (2001), Mars Global Surveyor Mars Orbiter Camera: Interplanetary cruise through primary mission, *J. Geophys. Res.*, *106*, 23,429–23,570, doi:10.1029/2000JE001455.

McEwen, A. S., et al. (2007), Mars Reconnaissance Orbiter's High Resolution Imaging Science Experiment (HiRISE), *J. Geophys. Res.*, *112*, E05S02, doi:10.1029/2005JE002605.

Milkovich, S. M., and J. W. Head III (2005), North polar cap of Mars: Polar layered deposit characterization and identification of a fundamental climate signal, *J. Geophys. Res.*, *110*, E01005, doi:10.1029/2004JE002349.

Milkovich, S., and J. Head (2006), Surface textures of Mars' north polar layered deposits: A framework for interpretation and future exploration, *Mars*, *2*, 21–45.

Milkovich, S. M., and J. J. Plaut (2008), Martian south polar layered deposit stratigraphy and implications for accumulation history, *J. Geophys. Res.*, *113*, E06007, doi:10.1029/2007JE002987.

Milkovich, S., J. Head, G. Neukum, and HRSC Co-Investigator Team (2008), Stratigraphic analysis of the northern polar layered deposits of Mars: Implications for recent climate history, *Planet. Space Sci.*, *56*, 266–288, doi:10.1016/j.pss.2007.08.004.

Milkovich, S. M., J. J. Plaut, A. Safaeinili, G. Picardi, R. Seu, and R. J. Phillips (2009), Stratigraphy of Promethei Lingula, south polar layered deposits, Mars, in radar and imaging data sets, *J. Geophys. Res.*, *114*, E03002, doi:10.1029/2008JE003162.

Murray, B., L. Soderblom, J. Cutts, R. Sharp, D. Milton, and R. Leighton (1972), Geologic framework of the south polar region of Mars, *Icarus*, *17*, 328–345, doi:10.1016/0019−1035(72)90004−8.

Perron, J., and P. Huybers (2009), Is there an orbital signal in the polar layered deposits on Mars?, *Geology*, *37*, 155–158, doi:10.1130/G25143A.1.

Phillips, R., et al. (2008), Mars north polar deposits: Stratigraphy, age, and geodynamical response, *Science*, *320*, 1182–1185, doi:10.1126/science.1157546.

Putzig, N., R. Phillips, B. Campbell, J. Holt, J. Plaut, L. Carter, A. Egan, F. Bernardini, A. Safaeinili, and R. Seu (2009), Subsurface structure of Planum Boreum from Mars Reconnaissance Orbiter Shallow Radar soundings, *Icarus*, *204*, 443–457, doi:10.1016/j.icarus.2009.07.034.

Tanaka, K., J. Rodriguez, J. Skinner, M. Bourke, C. Fortezzo, K. Herkenhoff, E. Kolb, and C. Okubo (2008), North polar region of Mars: Advances in stratigraphy, structure, and erosional modification, *Icarus*, *196*, 318–358, doi:10.1016/j.icarus.2008.01.021.

S. Byrne, Lunar and Planetary Laboratory, University of Arizona, 1629 E. University Blvd., Tucson, AZ 85721, USA.

K. E. Fishbaugh and P. S. Russell, Center for Earth and Planetary Studies, Smithsonian National Air and Space Museum, MRC 315, PO Box 30712, Washington, DC 20013, USA. (fishbaughke@si.edu)

K. E. Herkenhoff and R. Kirk, U.S. Geological Survey, 2255 N. Gemini Dr., Flagstaff, AZ 86001, USA.

C. S. Hvidberg and M. Winstrup, Center for Ice and Climate, Niels Bohr Institute, University of Copenhagen, Juliane Maries Vej 30, DK-2100 Copenhagen, Denmark.